



ORIGINAL ARTICLE

Amino-phenol complexes of Fe(III) as promising T_1 accelerators

Nikodem Kuźnik ^{a,*}, Marzena Wyskocka ^a, Magorzata Jarosz ^a, Lidia Oczek ^a, Sylwester Goraus ^a, Roman Komor ^a, Tomasz Krawczyk ^a, Marek Kempka ^b

^a Faculty of Chemistry, Silesian University of Technology, B. Krzywoustego 4, 44-100 Gliwice, Poland

^b Department of Macromolecular Physics, Adam Mickiewicz University, Umultowska 85, 61-614 Poznań, Poland

Received 2 July 2014; accepted 3 November 2014

Available online 7 November 2014

KEYWORDS

Fe(III) complexes;
Phenolates;
Salan ligand;
MRI contrast agents;
Relaxivity;
 T_1 relaxation time

Abstract Iron(III) complexes with N,O-ligands are compounds of high interest because they can be applied in catalysis and play an important role in living organisms, e.g., as models of catechol dioxygenase. Several N,O-ligands were studied: their synthesis, iron(III) complexation and the potential of the latter as T_1 -MRI contrast agents. A route to the tetrapodal N_3O_2 -naphthyl ligand was investigated. The resulting iron complex was obtained in 26% total yield and its relaxivity value was moderate ($r_1 = 1.03$ in water and $2.54 \text{ s}^{-1} \text{ mM}^{-1}$ in serum). Thus, phenyl isomeric salan complexes were obtained. These complexes differed in charge (positive and neutral) and in the presence of polar hydrogen-bonding substituents. The highest relaxivities ($r_1 = 2.39$ in water and $5.37 \text{ s}^{-1} \text{ mM}^{-1}$ in serum) were obtained for the Fe(III) cationic complex with MeO groups in the ligand. EPR studies confirmed a high spin configuration of rhombically distorted Fe(III) complexes.

© 2014 The Authors. Production and hosting by Elsevier B.V. on behalf of King Saud University. This is an open access article under the CC BY-NC-ND license (<http://creativecommons.org/licenses/by-nc-nd/3.0/>).

1. Introduction

Magnetic Resonance Imaging (MRI) has become a well-established technique in common medical practice. Contrast agents (CAs) are typically applied in over 40% of cases of MRI examinations (Que and Chang, 2009). The most widely used CAs are gadolinium complexes, however, manganese

compounds and hyperpolarized gases are also used (Caravan et al., 1999; Hermann et al., 2008). Iron, as the most abundant paramagnet in living organisms, is applied as ammonium iron(III) citrate (known as FAC) (Kivelitz et al., 1999) in T_1 -weighted imaging, while solid iron oxides are negative CAs (Wang, 2011). The quest for new CAs is spreading via various routes: smart CAs, bimodal agents (CT-MRIs), high relaxivity, unique selectivity, etc. (Caravan, 2009; Major and Meade, 2009; Pierre et al., 2014). Higher exploitation of endogenous metals (Mn, Fe) belongs to one of these routes (Schwert et al., 2002) since diseases such as nephrogenic systemic fibrosis (NSF), caused by the gadolinium species in the case of kidney dysfunction (Yerram et al., 2007), and environmental issues (Kümmerer and Helmers, 2000) obscure some of their potential advantages. The risk of lanthanide supply as

* Corresponding author. Tel.: +48 32 2371839; fax: +48 32 2372094.

E-mail address: Nikodem.Kuznik@polsl.pl (N. Kuźnik).

Peer review under responsibility of King Saud University.



Production and hosting by Elsevier

critical elements (European Commission, 2014) and environmental issues connected with gadolinium effluents (Kümmeler and Helmers, 2000) are of growing concern. Iron still remains underappreciated in this regard. Initial investigations of deferoxamine, EHPG and EHBG (Kuźnik et al., 2014; Richardson et al., 1999) systems found only a few successors: ParaCEST models (Dorazio and Morrow, 2012) and magnetization chameleons (Hasseroth, 2012) are the most advanced and up-to-date examples. We adapted Hasseroth's initial idea (Kuźnik et al., 2008; Touti et al., 2013) to Fe(III) complexes. Successful bioactivation of N,O,N-aminobis(phenol) ligands (Kuźnik et al., 2012) is currently being investigated for real iron complexes in steps. Aminophenol complexes, both with N,O,N-motifs and those based on a salan skeleton, exhibit poor redox activity which can additionally be tuned by the character of the ligand (Dean et al., 2012; Schmitt et al., 2002). Therefore, we investigated naphthalene derivatives, triphenol and diphenolpyridine systems as interesting T₁ accelerators of water protons. We compared a series of complexes with neutral and positive charge with an additional methoxy group which was introduced in order to enhance the desired interactions with the water molecules. Here, we would like to present studies covering the synthesis of ligands, their complexation and characteristics of the products.

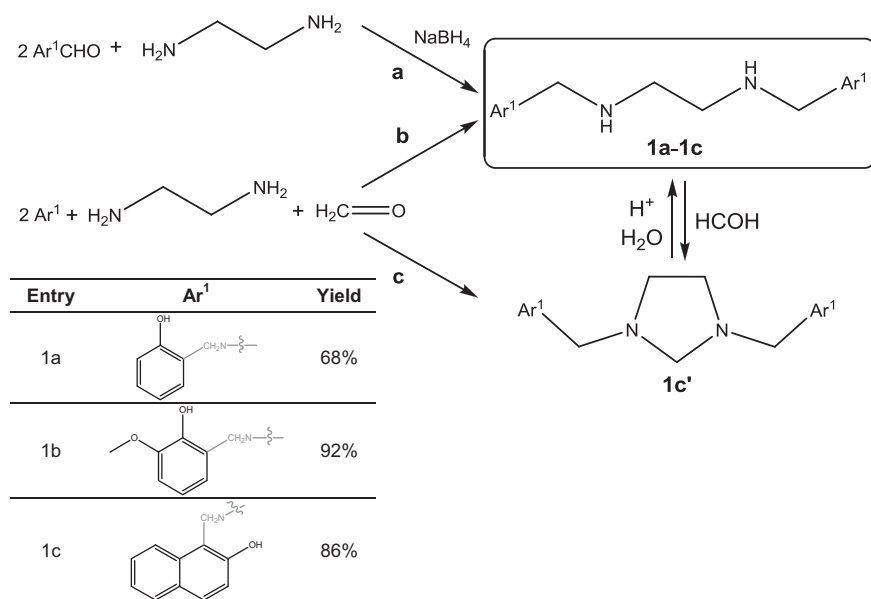
2. Results and discussion

Disubstituted ethylenediamines **1a–1c** were synthesized *via* two alternative pathways. Route *a* was applied for phenol (Ar¹) and its 2-methoxyderivative (Schmitt et al., 2002) – Scheme 1. The appropriate salens were reduced with NaBH₄. The Mannich reaction was applied according to route *b* for 2-naphthalene (Ar¹) – a method patented by Adamek was applied for the ethanolamine analog (Adamek and Bobulova, 1968). Two products were identified in the precipitate after 24 h of the reaction. According to the assigned NMR signals the mixture was

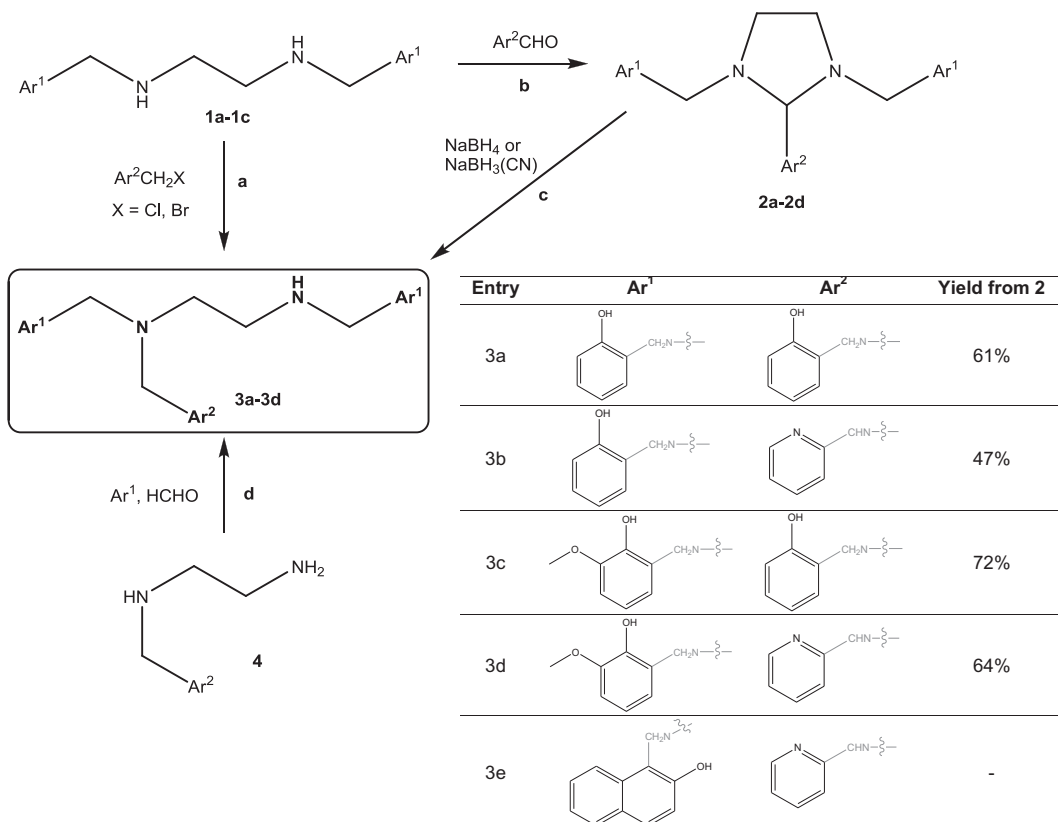
composed in 40% of the expected product **1c** and 60% of imidazolidine **1c'** as a product of consecutive formaldehyde addition to product **1c**. It was predictable that this reaction would occur because a secondary amine tends to be more nucleophilic than the substrate. However, during repetition of the reaction in 72 h the contribution of side product **1c'** dropped to 16% and the rest was composed purely of the desired product **1c**.

The recovery of **1c** from **1c'** is regarded as hydrolysis under acidic conditions (Fife et al., 1978). Weakly acidic naphthalene may catalyze such a reaction. Thus, a prolonged reaction time is recommended in order to achieve thermodynamic equilibrium. Nevertheless the methods were found to be very convenient since the pure products were collected as crystalline solids in high yields (70–96%). No other side products of any following alkylation reactions were observed.

Synthesis of the target ligands was designed *via* approaches *a–d* – Scheme 2. Compounds **3a–3d** were obtained *via* routes *b–c* according to Schmitt's work (Schmitt et al., 2002). After the addition of appropriate aldehydes (step *b*), imidazolidine intermediates were formed (**2a–2d**) which were then identified by both NMR and X-ray spectroscopy (Fig. 1); however, they were not separated from the reaction mixture as they were reduced *in situ* with NaBH₄ or NaBH₃(CN) and preceded by stoichiometric CCl₃COOH (**3a–3c**) or CF₃COOH (**3d**) addition instead. The reduction was carried out at a lower temperature because it proceeds rapidly at ambient temperature. Lowering the temperature was also done to prevent reverse hydrolysis and re-cyclization. Initially applied NaBH₄ turned out to lead to many by-products. However, its replacement with NaBH₃(CN) led to satisfactory results. Products of reduction **3a** precipitated from the reaction mixture as crystal solids of sufficient purity. This is the next advantage which makes the synthesis very convenient. An alternative route, *a*, was studied for **3b**. Both (2-pyridyl)methyl chloride and bromide were checked. Fivefold molar excess of diamine **1a** was applied in order to limit the following *N*-alkylation of the diamine.



Scheme 1 Synthesis and yields of 1,2-substituted ethane-1,2-diamines **1a–1c**. (a) MeOH, r.t., NaBH₄, 1.5 h, (b) MeOH, r.t., 72 h, (c) MeOH, r.t., 24 h.



Scheme 2 Synthesis of **3a–3d** ligands. (a) MeOH, NaHCO₃, reflux, (b) MeOH, r.t., (c) MeOH, Cl₃CCOOH in 0 °C, then NaBH₄ or NaBH₃CN, (d) MeOH, r.t.

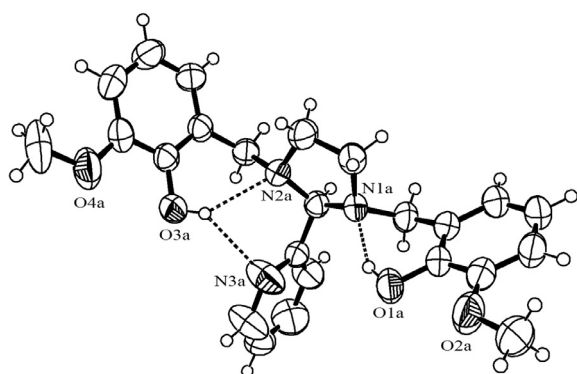
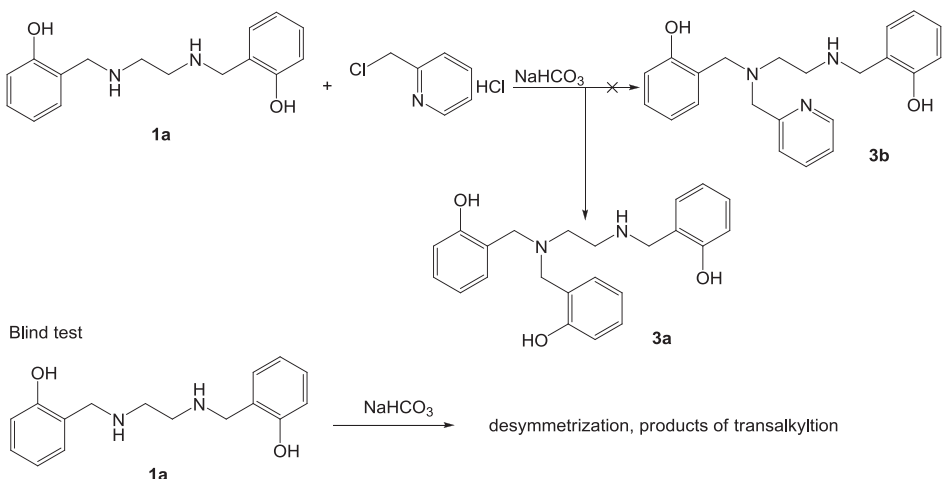
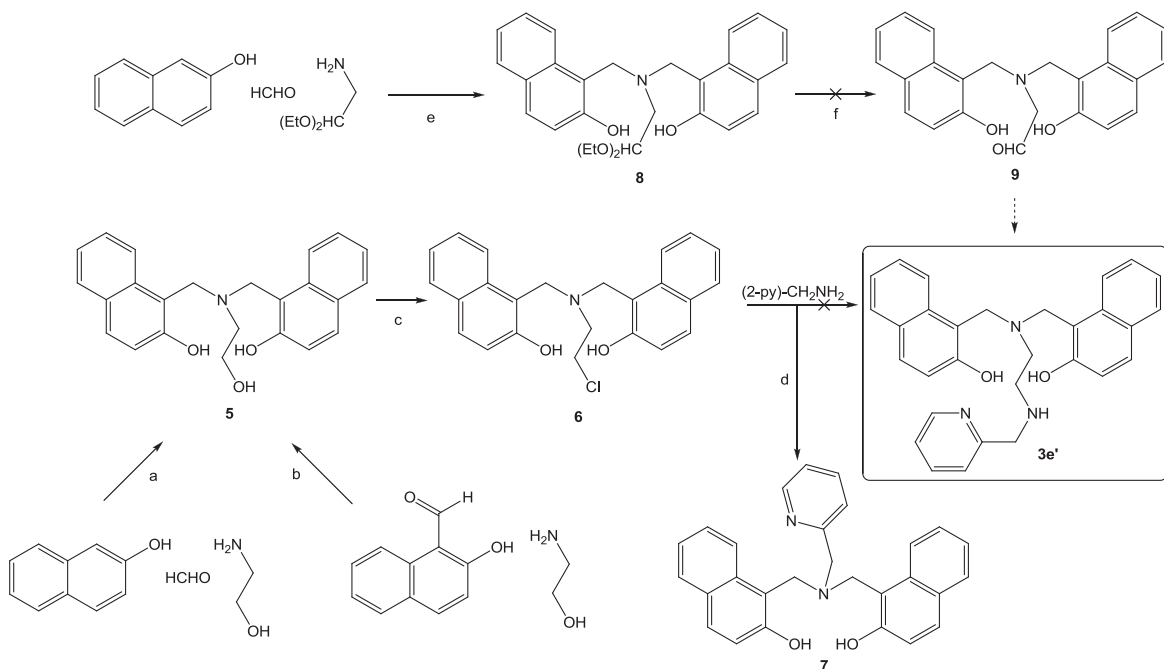


Figure 1 X-ray structure of 2-(2-pyridyl)-1,3-bis(2-hydroxy-3-methoxybenzyl)imidazolidine (**2d**), 60% probability ellipsoids, H-bonds presented with a dashed line.

Nevertheless, this method gave worse results (26% and 6% yield, respectively). Moreover, a major product observed in this reaction was in fact **3a**, i.e., the product of the intermolecular transfer of the Ar¹CH₂-fragment (**Scheme 3**). We performed a blind test by heating **1b** with NaHCO₃ to mimic conditions from route *a* (from **Scheme 2**) and we observed complete desymmetrization of the initial symmetric **1b** system (**Scheme 3**), thus concluding that these conditions promote intermolecular transalkylation. Thus method *b–c* was chosen as the most selective for the synthesis of ligand.

We tried to synthesize the naphthol derivative **3e** via the *b–c* route (**Scheme 2**), however, instead of the expected product **3e**, disubstitution of an aldehyde to each of the amine centers was observed. Large naphthol substituents constitute a steric hindrance and hamper formation of the cyclic intermediate **2**. Therefore, we turned back to the isomeric structure **3e'** (**Scheme 4**) using the method described earlier for the plain phenol counterpart (Kuźnik et al., 2012). Reductive amination *b* was not successful, but we did manage to synthesize compound **5** in the Mannich reaction *a*. We also managed to convert it into its chloroderivative **6**. However, final substitution with 2-aminemethylpyridine did not result in the desired product **3e'**, only the tertiary amine **7** was observed. Therefore, we applied milder conditions in order to avoid elimination of the ethylene bridge, yet this did not help. Although we did not observe any aziridine formation in the case of the phenyl analog, here it is the most likely explanation for the ethylene elimination. Even mild basic conditions might favor the formation of the aziridinium cation as a competitive reaction to Cl intermolecular substitution. Bulky naphthalene substituents may impede the attack of the primary pyridyl amine. Finally, another optional approach was considered – the Mannich reaction of 2-naphthol with formaldehyde and 2,2-diethoxyethanamine. This approach led to the expected acetal-protected aldehyde **8**. Its formation was confirmed by X-ray analysis (**Fig. 2**). However, the following reaction of deprotection leading to aldehyde **9** was never successful. Various conditions, solvents and catalysts were tested, but none of them proved to be successful. Stabilization of the acetal might be explained by a highly hydrophobic surrounding of the methine position.

Scheme 3 Transalkylation occurring during *N*-alkylation.Scheme 4 Synthetic approaches to *N,N*-bis[1-(2-hydroxynaphthyl)methyl]-*N'*-(2-pyridylmethyl)ethane-1,2-diamine (3e') (a) MeOH, r.t., 48 h, (b) MeOH, r.t., NaBH₄, (c) CH₂Cl₂, SOCl₂, saturated solution of Na₂CO₃, 24 h, (d) EtOH, r.t., 48 h, (e) MeOH, r.t., 48 h, (f) HCl (6 M) or TFA/H₂O.

2.1. X-ray structures

2-(2-Pyridyl)-1,3-bis(2-hydroxy-3-methoxybenzyl)imidazolidine (**2d**) crystallizes in the triclinic P-1 space group with 6 molecules in the unit cell (Fig. 1). The pyridyl ring is twisted out from an average plane of the remaining rings. The hydroxyl group O3A-H forms an intramolecular hydrogen bonding to two nitrogen acceptors: N2A (2.23 Å) and N3A (2.38 Å). Another intramolecular hydrogen bond was found for O1A-H...N1A (1.91 Å). The saturated five-membered ring of the imidazolidine moiety is clearly visible, which is in agreement with NMR data.

N,N-Bis[1-(2-hydroxynaphthyl)methyl]-2,2-diethoxyethanamine (**8**) crystallizes in the monoclinic C2/c space group with

8 molecules in the unit cell (Fig. 2). In this case *zwitterion* was not found in the crystal structure, although flexible ethoxy groups were observed. Two hydrogen bonds were found for this structure: an intramolecular strong bond for O1A-H...N1 (1.56 Å) and an intermolecular O1B-H...O1A (1.77 Å).

Bis(2-hydroxybenzyl)amine (**3f**) crystallizes in the monoclinic P2₁/c space group with 4 molecules in the unit cell (Fig. 3). It forms a *zwitterionic* internal salt as a result of proton transfer from the hydroxyl group (O5) to the nitrogen atom of the secondary amine. There is one intramolecular hydrogen bond N1-H...O5 (2.09 Å) with the deprotonated phenolate oxygen atom. There is also a network of intermolecular hydrogen bonding. It consists of one pair of O5...H-N1

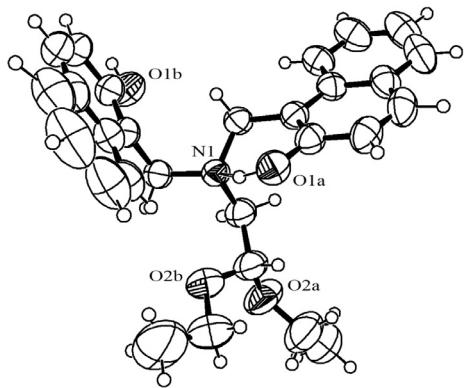


Figure 2 X-ray structure of *N,N*-bis[1-(2-hydroxynaphthyl)methyl]-2,2-diethoxyethanamine (8) 60% probability ellipsoids. Intramolecular hydrogen bond O1A-H...N1 is not shown.

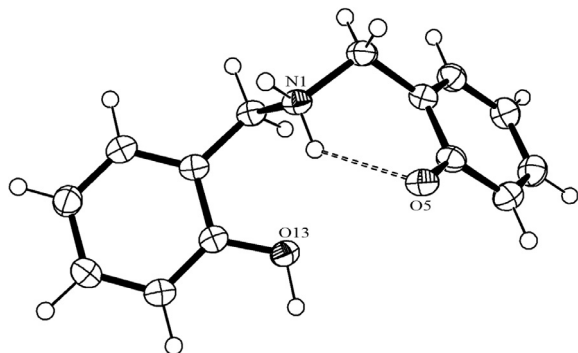


Figure 3 X-ray structure of bis(2-hydroxybenzyl)amine (3f), 60% probability ellipsoids. H-bonds presented with a dashed line.

(1.62 Å) and O13-H...O5 (1.51 Å) for two interacting molecules and a reverse combination.

2.2. Synthesis and structure of the complexes

Appropriate Fe(III) complexes (**4a–4d**, respectively) were obtained in a reaction of iron(III) chloride or perchlorate with the obtained ligands **3a–3d**. This step was followed by the deprotonation of OH groups with NaOH. Small excess (10%) of the ligand prevented the precipitation of Fe(OH)₃. Crude products precipitated and were purified on column chromatography or at least by washing with water followed by diethyl ether. Marvilliers presented an X-ray structure of ligand **3b** with chloride in the sixth coordination site (Marvilliers and Poussereau, 2002). We studied our samples with mild MS ionization but there were no other signals than those assigned to complex **4b** ions. We also investigated the possibility of direct Cl coordination to Fe for other complexes but found no proof for this hypothesis. Unfortunately, we did not succeed in obtaining the appropriate fine crystals for X-ray analysis. Additionally, the Fe(III) complex with bis(2-hydroxybenzyl)amine (**3f**) – Na[Fe(3f)₂] was synthesized as a structurally related reference compound, but having a saturated coordination sphere.

Table 1 Relaxivities of complexes.

Complex	r_1 [mM ⁻¹ s ⁻¹] in H ₂ O 300 MHz ^a	r_1 [mM ⁻¹ s ⁻¹] in H ₂ O 16.5 MHz ^b	r_1 [mM ⁻¹ s ⁻¹] in serum 300 MHz ^a
4a [Fe(3a)]	1.75	0.85	2.75
4b [Fe(3b)] ⁺	1.97	1.09	2.95
4c [Fe(3c)]	2.10	1.22	3.08
4d [Fe(3d)] ⁺	2.39	1.39	5.37
4e [Fe(3e)] ⁺	1.03	–	2.54
4f [Fe(3f)] [–]	0.16	–	0.10

^a Measured at 300 MHz, 7.1 T, 22 °C.

^b Measured at 16.5 MHz, 0.4 T, 37 °C.

2.3. Properties of the complex

Relaxivity measurements. T_1 measurements were performed for purified complexes **4a–4f**. The appropriate relaxivity values are given in Table 1. Relaxivity is arranged in growing order from a neutral complex with unsubstituted salan ligand **4a** – [Fe(3a)]¹ to the cationic complex with the additional methoxy group on ligand **4d** – [Fe(3d)]⁺. It was found that changing the character from neutral to cationic enhances the resulting relaxivity. However, it was interesting to find that the presence of the MeO-group on the ligand (**4c**, [Fe(3c)]) raised relaxivity more than the cationic character (**4b** [Fe(3b)]⁺ in comparison to **4a** [Fe(3a)]). As designed, the MeO-group increased relaxivity and the effect may have come from H-bond interactions increasing the outer-sphere mechanism of proton relaxation enhancement (PRE) or by influencing one of the factors in the inner sphere (Lauffer, 1987). The latter could be that the rotation correlation time was only a steric parameter, while the water exchange rate could be the result of the group's electron-donating character. But Margerum observed a lower rate of exchange of water molecules for strong electron donors (Margerum et al., 1978), so we suspect that steric and polar effects dominate in this case. A serious increase of relaxivity was observed in the serum. The r_1 values were doubled as a result of higher viscosity of the medium and of receptor-induced magnetization enhancement (RIME). Such high values are comparable with the commonly used gadolinium contrast agents (Geraldes and Laurent, 2009). Complex **4f** with the naphthyl rings did not meet our expectations. Its relatively low relaxivity in aqueous solutions was not surprising since highly hydrophobic large naphthyl rings could be a barrier for polar water molecules and thus resulted in less efficient water interactions. However, we did expect an increase in relaxivity in serum and it was doubled as compared with the aqueous solution but still lower than any of the phenyl complexes **4a–4d**. Perhaps substitution of the rings with Cl[–] or Br[–] would enhance affinity to human serum albumin and increase the relaxivity, as it did for the Fe(III)-EHPG derivatives (Lauffer et al., 1987). Complex **4f** [Fe(3f)₂][–] with a saturated coordination sphere and non-polar substituent was measured as a reference to show the impact of direct water interaction with a paramagnet in the other models. An intriguing relationship could be found between the two series of measurements at 16.5 and 300 MHz. The trends were consistent at both

¹ The ligands **3a–3f** are in the deprotonated form in the complexes; i.e., the abbreviation [Fe(3a)] concerns an iron(III) complex **4a** with the deprotonated ligand **3a**.

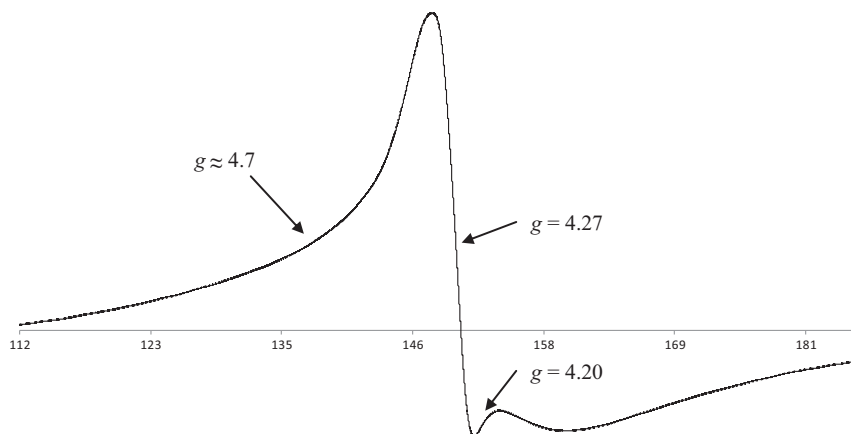


Figure 4 EPR spectrum for **4a** representing a typical spectrum for all **4a–4d** complexes. Measured in frozen MeOH (78 K). Instrument parameters: modulation freq. 100 kHz, power 0.5 mW, mod. width 1 mT, amplitude 100, time const. 0.1 s, sweep time 4×1 min, complex concentration 1 mM.

frequencies of the magnetic field, but the relaxivities at higher frequency outweighed those at the low field. This is not a typical behavior, although it could be explained on the basis of the Bloembergen theory (Bloembergen, 1957). One of the relaxivity factors is the spin relaxation time τ_S – a field-dependent parameter. For iron it is short as compared to proton relaxation (10^{-2} – 10^0 s) but it has a broad range of 10^{-10} – 10^{-12} s. Generally, the shorter the τ_S , the higher the magnetic field for the optimal relaxivity. Thus we suspect that the iron complexes are suitable CAs for higher magnetic fields as opposed to classical gadolinium contrast agents. This feature is positive since one of the development directions in MRI medical scanners is increasing the magnetic field.

EPR spectra of complexes **4a–4d** show two signals – Fig. 4. The measurement was performed to assess the magnetic state and geometry of the products.

The major signal at $g = 4.27$ could be assigned to the middle and lower Kramer's doublet rhombically distorted high-spin Fe(III) complex. It is observed for most high-spin Fe(III) phenolate complexes, while the minor signal at $g = 4.20$ and a broad shoulder $g \approx 4.7$ could be assigned to weak resonance of the ground Kramer's doublets in the axial symmetry.

3. Conclusions

Driven by several arguments, such as the quest for gadolinium contrast agent supplements and alternatives, we synthesized new Fe(III)-N,O,N and Fe(III)-salan complexes and measured their acceleration of water proton relaxation (T_1). Our initial attempts did not lead us to the expected N,O,N-ligand **3e'**. The isomeric salan skeleton of the naphthyl ligand was obtained in a relatively low yield, but the resulting complex had moderate relaxivities. Much better results in the synthesis, purification and PRE properties were found for the phenyl counterparts. These were studied in a series of different charges and with additional MeO substituents. The highest relaxivity values were found for the positively charged methoxy derivative **4d**, which is already at the level of gadolinium contrast agents.

The tested compounds only had a value of model CAs. We were fully aware of the concerns regarding redox activity of

iron compounds, especially those with a free coordination site. This gap leads to high relaxivities, not yet reported for iron compounds, but could also be a pitfall. Kozak showed the irreversible character of the redox processes for Fe(III)-N,O,N complexes, which is more likely connected with ligand electron transfer (Dean et al., 2012). On the other hand, Schmitt showed instability seen on MS spectra for respective Mn-salan complexes (Schmitt et al., 2002) which was not observed in our models. Nevertheless, comprehensive redox studies are our main priority in the nearest future. In the case of redox activity we are currently considering two approaches, e.g., the introduction of bulky alkene substituents (*t*-Bu, Cy) in order to limit interaction of the central atom with the smallest molecules, such as water. Relaxivity of the complexes should also benefit from this direction. Alternatively, we plan to introduce the carboxyl group into the ligand or other groups less prone to oxidation thus affecting the redox processes.

4. Experimental

All liquid chemicals and solvents were dried and distilled prior to use. NMR spectra were taken on Agilent 400 and 600 MHz spectrometers using solvent signal as an internal reference at room temperature. Electrospray-ionization mass spectrometry was performed on a 4000 QTrap (Applied Biosystems/MDS Sciex) mass spectrometer. High resolution mass spectra were registered on a Micromass/Waters LCT (TOF) spectrometer at the University of Warsaw. Relaxivity: T_1 has been measured on Varian Unity Inova 300 MHz spectrometer using Inversion Recovery (IR) sequence at 20 °C with $t_1 = 15$ s and t_2 : 0.05, 0.1, 0.5, 0.75, 1, 3 s. The samples of complexes at concentrations: 0.3, 0.6, 0.9 and 1.2 mmol/dm³ were dissolved in 5% D₂O and 10% DMSO in H₂O mixture and degassed by nitrogen purging. Longitudinal relaxation time measurements at low frequency for sample concentrations 0, 0.15, and 0.3 mmol/dm³ were gathered using home-made Spin-Echo spectrometer, operating at 16.5 MHz. The spectrometer is equipped with an NMR magnet field stabilizer (10 Hz field stability), sample temperature stabilizer (0.2 °C resolution) and Pulsed Field Gradient Unit (120 Gs/cm max value of z-gradient) for self-diffusion experiment. IR method has been

employed to obtain the longitudinal relaxation time T_1 for studied samples. Each sample was placed in spectrometer probe head for half an hour before the measurements were collected in order to equilibrate the temperature, i.e., 37 °C. The IR sequence consisted of 16 tau values, exponentially distributed over 5 T_1 range – they have been selected in a preliminary run and used in the final measurement for each sample. The sequence was executed approximately within the 5 T_1 period and the successive scans of FID signal were accumulated ($N = 4$) for the S/N enhancement. The measured values of T_1 represent mean value from 3 measurements with the maximal uncertainty of 3%. Based on a $1/T_1$ vs. C plot, the slope was calculated as a relaxivity value with an appropriate error. EPR measurements were recorded on JEOL JES-FA200 spectrometer. The samples were dissolved in methanol, a capillary cuvette was used; the measurements were conducted at 78 K. IR spectra were registered on Nicolet 6700 ATC-FTIR spectrophotometer. *N,N*-Bis(2-hydroxybenzyl)amine (**3f**) was obtained according to the Searcey's method from salicyl oxime (Searcey et al., 2003). Elemental analysis was performed in the Silesian University of Technology. Tables of bond distances and angles, atomic coordinates, and anisotropic thermal parameters for **2d**, **3f** and **8** have been deposited at the Cambridge Crystallographic Data Centre, respective No.: CCDC 991614, 991615, 991616. A complete listing of the atomic coordinates can be obtained free of charge, on request, from the Director, Cambridge Crystallographic Data Centre, 12 Union Road, Cambridge CB2 1EZ, UK [fax: (+Int) 44–1223 336 033; email: deposit@ccdc.cam.ac.uk], on quoting the depository numbers, the names of the authors, and the journal citation.

4.1. Crystal data for 2-(2-pyridyl)-1,3-bis(2-hydroxy-3-methoxybenzyl)imidazolidine (**2d**)

The crystal chosen for X-ray analysis was a clear yellowish prism with the approximate dimensions $1.0 \times 0.5 \times 0.5$ mm. $C_{24}H_{27}N_3O_4$ (421.49 g mol⁻¹) crystallizes in the triclinic system, space group P-1, with $a = 14.366$ (3), $b = 15.515$ (3), $c = 16.075$ (3) Å, $\alpha = 81.55$ (3), $\beta = 87.39$ (3), $\gamma = 67.80$ (3) °, $V = 3280.9$ (11) Å³, $Z = 6$, $\mu(\text{MoK}\alpha) = 0.088$ mm⁻¹, and $D_{\text{calcd}} = 1.280$ cm⁻³. A total of 11,575 reflections were collected to $2\Theta_{\text{max}} = 50.17$ ° ($h: -15 \rightarrow 16$, $k: 0 \rightarrow 17$, $l: -18 \rightarrow 19$), of which 11,096 were unique. In refinements, weights were used according to the scheme $w = 1/[\sigma^2(F_o^2) + (0.1385P)^2]$, where $P = (F_o^2 + 2F_c^2)/3$. The refinement of 867 parameters converged to the final agreement factors $R = 0.0610$ for 7127 reflections with $F_o > 4\sigma$ (F_o) and $R_w = 0.1974$, and $S = 1.050$ for all observed reflections. The electron density of the largest difference peak was found to be 0.38 e Å⁻³, while that of the largest difference hole was -0.30 e Å⁻³.

4.2. Crystal data for bis(2-hydroxybenzyl)amine (**3f**)

The crystal chosen for X-ray analysis was a clear red needle with the approximate dimensions $0.4 \times 0.07 \times 0.07$ mm. $C_{14}H_{15}NO_2$ (229.27 g mol⁻¹) crystallizes in the monoclinic system, space group P2₁/c, with $a = 8.0226$ (5), $b = 6.8910$ (4), $c = 21.6719$ (15) Å, $\beta = 95.026$ (6), $V = 1193.50$ (13) Å³, $Z = 4$, $\mu(\text{CuK}\alpha) = 0.687$ mm⁻¹, and $D_{\text{calcd}} = 1.276$ cm⁻³.

A total of 4268 reflections were collected to $2\Theta_{\text{max}} = 73.75$ ° ($h: -9 \rightarrow 9$, $k: -5 \rightarrow 8$, $l: -26 \rightarrow 25$), of which 2271 were unique. In refinements, weights were used according to the scheme $w = 1/[\sigma^2(F_o^2) + (0.0577P)^2 + 0.3049P]$, where $P = (F_o^2 + 2F_c^2)/3$. The refinement of 214 parameters converged to the final agreement factors $R = 0.0441$ for 1873 reflections with $F_o > 4\sigma$ (F_o) and $R_w = 0.1218$, and $S = 1.060$ for all observed reflections. The electron density of the largest difference peak was found to be 0.23 e Å⁻³, while that of the largest difference hole was -0.21 e Å⁻³.

4.3. Crystal data for *N,N*-bis[1-(2-hydroxynaphthyl)methyl]-2,2-diethoxyethanamine (**8**)

The crystal chosen for X-ray analysis was a clear pale red block with the approximate dimensions $0.15 \times 0.1 \times 0.1$ mm. $C_{28}H_{31}NO_4$ (445.54 g mol⁻¹) crystallizes in the monoclinic system, space group C2/c, with $a = 19.010$ (4), $b = 7.9776$ (16), $c = 32.345$ (7) Å, $\beta = 93.16$ (3), $V = 4897.8(17)$ Å³, $Z = 8$, $\mu(\text{CuK}\alpha) = 0.641$ mm⁻¹, and $D_{\text{calcd}} = 1.208$ cm⁻³. A total of 15,362 reflections were collected to $2\Theta_{\text{max}} = 74.33$ ° ($h: -23 \rightarrow 16$, $k: -9 \rightarrow 9$, $l: -40 \rightarrow 39$), of which 4856 were unique. In refinements, weights were used according to the scheme $w = 1/[\sigma^2(F_o^2) + (0.0977P)^2 + 1.4980P]$, where $P = (F_o^2 + 2F_c^2)/3$. The refinement of 382 parameters converged to the final agreement factors $R = 0.0560$ for 3802 reflections with $F_o > 4\sigma$ (F_o) and $R_w = 0.1794$, and $S = 1.011$ for all observed reflections. The electron density of the largest difference peak was found to be 0.26 e Å⁻³, while that of the largest difference hole was 0.19 e Å⁻³.

4.4. *N,N*-Bis(2-hydroxybenzyl)amine iron(III) sodium complex (**4f**, $Na[Fe(\mathbf{3f})_2]$)

A suspension of *N,N*-bis(2-hydroxybenzyl)amine (**3f**) 200 mg (0.875 mmol) in hot methanol (2 cm³) was prepared. It was alkalinized with aqueous 0.5 M NaOH solution (7 cm³), then left for 0.5 h. After cooling aqueous $FeCl_3$ (141 mg, 0.875 mmol in 3.5 cm³ water) solution was added. A dark brown precipitate was observed. The reaction mixture was put in refrigerator. Next day, after evaporation of volatiles, the residue was washed with methanol (3 × 15 cm³) and purified on a reversed phase column eluting with acetonitrile/water 1:1 mixture. 163 mg, 0.321 mmol, 37% of pure product was obtained as a brown solid. *IR* (cm⁻¹): 1268 s ($\nu_{C=O}$); 2594 m, 1478 s ($\nu_{C-Ar-CAr}$); 1032–1150 s-m (ν_{C-N}); 752 vs. (1,2-disubstituted aromatic). *MS-ESI* (m/z): 510.3 ([M–Na]⁺). For $C_{28}H_{26}FeN_2NaO_4$ calculated C 63.0 H 4.9 N 5.2 found C 62.7 H 5.1 N 5.5%.

4.5. *N,N'*-Bis[(2-hydroxyphenyl)methyl]ethan-1,2-diamine (**1a**)

Methanol (75 cm³), salicylaldehyde 5.2 cm³ (50 mmol), ethan-1,2-diamine 1.7 cm³ (25 mmol) were introduced into a round-bottomed flask. Mixture turned immediately yellow and a precipitate appeared. Reaction mixture was kept under stirring for 1 h at room temperature. Small portions of sodium borohydride 1.89 g (50 mmol) were introduced, stirred for next 0.5 h and then kept in a fridge for 2 h. The obtained white precipitate was filtered off on fritted funnel, washed with cold

methanol, dried and recrystallized from methanol (4.61 g, 16.9 mmol, 68%). ¹H NMR (600 MHz, CDCl₃): δ 2.84 (s, 4H, NH-CH₂-CH₂-NH), 3.99 (s, 4H, Ar-CH₂-NH), 6.78 (td, 2H, J = 7.2 Hz, 1.2 Hz, H-C₅), 6.83 (d, 2H, J = 7.8 Hz, H-C₃), 6.98 (dd, 2H, J = 7.2 Hz, 1.2 Hz, H-C₆), 7.17 (t, 2H, J = 7.8 Hz, H-C₄). ¹³C{¹H} NMR (600 MHz, CDCl₃): δ 47.8 (NH-CH₂-CH₂-NH), 52.6 (Ar-CH₂-NH), 116.3 (C₄), 119.2 (C₆), 122.1 (CH₂-C₁), 128.4 (C₃), 128.9 (C₅), 157.9 (OH-C₂). mp = 124 °C.

4.6. N,N'-Bis[(2-hydroxy-3-methoxyphenyl)methyl]ethan-1,2-diamine (1b)

Methanol (75 cm³), 2-hydroxy-3-methoxybenzaldehyde (*ortho*-Vanilin) 7.61 cm³ (50 mmol), ethan-1,2-diamine 1.7 cm³ (25 mmol) were introduced into a round-bottomed flask. The mixture turned orange immediately and a precipitate appeared. The reaction mixture was kept under stirring for 1 h at room temperature. Small portions of sodium borohydride 1.89 g (50 mmol) were introduced, stirred for next 0.5 h and then kept in a fridge for 2 h. The resulting white precipitate was filtered off on fritted funnel, washed with cold methanol, and dried (7.62 g, 22.9 mmol, 92%). ¹H NMR (600 MHz, CDCl₃): δ 2.82 (s, 4H, NH-CH₂-CH₂-NH), 3.87 (s, 6H, CH₃-O), 3.98 (s, 4H, Ar-CH₂-NH), 6.62 (d, 2H, J = 7.9 Hz, H-C₄), 6.74 (dd, 2H, J = 7.9 Hz, H-C₅), 6.81 (d, 2H, J = 7.9 Hz, H-C₆). ¹³C{¹H} NMR (600 MHz, CDCl₃): δ 47.7 (NH-CH₂-CH₂-NH), 51.9 (Ar-CH₂-NH), 55.9 (CH₃-O), 110.9 (C_{Ar}), 118.8 (C_{Ar}), 120.7 (C_{Ar}), 122.8 (CH₂-C_{Ar}), 146.8 (OH-C_{Ar}), 147.9 (CH₃-O-C_{Ar}). mp = 167–168 °C.

4.7. N,N'-Bis[(2-hydroxy-1-naphthyl)methyl]ethan-1,2-diamine (1c)

Methanol (25 cm³), 2-naphthol 2.88 g (20 mmol), ethan-1,2-diamine 0.7 cm³ (10 mmol) and formaldehyde 37% 1.6 cm³ (20 mmol) were introduced into a round-bottomed flask. The mixture warmed up and a pale orange precipitate appeared. The reaction mixture was kept under stirring for 72 h at room temperature. The product obtained was filtered off on a fritted funnel and dried (3.21 g, 8.62 mmol, 86%). ¹H NMR (600 MHz, CDCl₃): δ 2.97 (s, 4H, NH-CH₂-CH₂-NH), 4.48 (s, 4H, Ar-CH₂-NH), 7.1 (d, 2H, J = 9 Hz, Ar), 7.29 (t, 2H, J = 7.2 Hz, Ar), 7.41 (t, 2H, J = 7.8 Hz, Ar), 7.69 (d, 2H, J = 9 Hz, Ar), 7.73–7.76 (m, 4H, Ar). ¹³C{¹H} NMR (600 MHz, CDCl₃): δ 47.3 (NH-CH₂-CH₂-NH), 48.0 (Ar-CH₂-NH), 110.0 (C_{Ar}), 111.6 (C_{Ar}), 119.4 (C_{Ar}), 120.9 (C_{Ar}), 122.5 (C_{Ar}), 126.4 (C_{Ar}), 128.9 (C_{Ar}), 129.3 (C_{Ar}), 132.4 (C_{Ar}), 156.6 (C_{Ar}). MS-ESI (*m/z*): 371.4 [M-H⁺]⁺, HRMS /M-H⁺J⁺: for C₂₄H₂₃N₂O₂ calculated 371.1760, found 371.1775, mp = 139–141 °C.

4.8. N,N,N'-Tris[(2-hydroxyphenyl)methyl]ethan-1,2-diamine (3a) (Schmitt et al., 2002)

Methanol (30 cm³), N,N'-bis[(2-hydroxyphenyl)methyl]ethan-1,2-diamine (1a) 1.36 g (5 mmol) and salicylaldehyde 0.53 cm³ (5 mmol) were introduced into a round-bottomed flask. The mixture was refluxed for 1.5 h. Then the reaction mixture was cooled at an ice-salt bath while stirring. Trichloroacetic acid 0.820 g (5 mmol) was added to the pale yellow

reaction mixture and next sodium borohydride 0.306 g (8.1 mmol) was introduced in small portions. The reaction mixture was kept in an ice bath for an hour, then at room temperature for the following hour. A white precipitate appeared. Post-reaction mixture was put into the refrigerator overnight. The resulting white precipitate was filtered off on a fritted funnel, washed with cold methanol and dried. (1.15 g, 3.05 mmol, 61%). ¹H NMR (600 MHz, CDCl₃): δ 2.53 (t, 2H, J = 6 Hz, CH₂-CH₂-NH), 2.72 (t, 2H, J = 6 Hz, N-CH₂-CH₂), 3.56 (s, 4H, Ar-CH₂-N), 3.64 (s, 2H, Ar-CH₂-NH), 6.59 (td, 1H, J = 7.8, 1.2 Hz, Ar), 6.37 (dd, 1H, J = 8.4, 1.2 Hz, Ar), 6.64 (td, 2H, J = 7.2, 1.2 Hz, Ar), 6.69 (dd, 1H, J = 8.4, 0.6 Hz, Ar), 6.74 (dd, 2H, J = 7.8, 1.2 Hz, Ar), 6.92 (dd, 2H, J = 7.2, 1.8 Hz, Ar), 6.95–7.02 (m, 2H, Ar). ¹³C{¹H} NMR (400 MHz, CDCl₃): 45.2 (CH₂-CH₂-NH), 51.4 (N-CH₂-CH₂), 52.1 (Ar-CH₂-NH), 56.1 (Ar-CH₂-N), 116.2 (C_{Ar}), 116.5 (C_{Ar}), 119.3 (C_{Ar}), 120.0 (C_{Ar}), 122.5 (C_{Ar}), 122.6 (C_{Ar}), 128.8 (C_{Ar}), 128.9 (C_{Ar}), 129.4 (C_{Ar}), 130.4 (C_{Ar}), 155.9 (C_{Ar}), 157.6 (C_{Ar}). mp = 177–178 °C. For C₂₃H₂₆N₂O₃ calculated C 73.0 H 6.9 N 7.4 found C 72.9 H 7.2 N 7.5%.

4.9. N,N'-Bis[(2-hydroxyphenyl)methyl]-N'-[(2-pyridyl)methyl]ethane-1,2-diamine (3b)

The compound was obtained as a modification of Marvilliers' method (Marvilliers and Poussereau, 2002). Methanol (30 cm³), N,N'-bis[(2-hydroxyphenyl)methyl]ethan-1,2-diamine (1a) 1.36 g (5 mmol) and 2-pyridine carboxyaldehyde 0.5 cm³ (5 mmol) were introduced into a round-bottomed flask. The mixture was refluxed for 2 h. Then the reaction mixture was cooled in an ice-salt bath while stirring. Trichloroacetic acid 0.821 g (5 mmol) was added to the reaction mixture and next sodium cyanoborohydride 0.510 g (8.1 mmol) was introduced in small portions. The reaction mixture was kept in ice bath for 2 h, then at room temperature for 24 h. All the volatiles were evaporated on a rotary evaporator and the resulting brown oily residue was dissolved in 5 cm³ chloroform, washed with water (10 cm³) and the aqueous layer was extracted with chloroform (3 × 5 cm³). The organic phases were combined, dried over anhydrous magnesium sulfate and evaporated on a rotary evaporator. The product was obtained as yellow oil (0.848 g, 2.33 mmol, 47%). ¹H NMR (400 MHz, CDCl₃): δ 2.90 (m, 4H, CH₂-CH₂-NH and N-CH₂-CH₂), 3.71 (s, 2H, Py-CH₂-N), 3.83 (s, 2H, Ar-CH₂-N), 3.91 (s, 2H, Ar-CH₂-NH), 6.76–6.86 (m, 4H, Ar), 7.00 (t, 2H, J = 6.8 Hz, Ar) 7.01–7.21 (m, 4H, Ar), 7.63 (t, 1H, J = 7.6 Hz), 8.32 (d, 1H, J = 4.4 Hz). ¹³C{¹H} NMR (400 MHz, CDCl₃): 44.9 (CH₂-CH₂-NH), 48.9 (N-CH₂-CH₂), 50.5 (Py-CH₂-N), 57.9 (Ar-CH₂-N), 58.2 (Ar-CH₂-NH), 116.4 (C_{Ar}), 116.6 (C_{Ar}), 118.5 (C_{Ar}), 119.7 (C_{Ar}), 119.9 (C_{Ar}), 122.5 (C_{Ar}), 122.9 (C_{Ar}), 123.5 (C_{Ar}), 129.5 (C_{Ar}), 130.2 (C_{Ar}), 130.3 (C_{Ar}), 130.5 (C_{Ar}), 137.7 (C_{Ar}), 148.3 (C_{Ar}), 156.2 (C_{Ar}), 156.9 (C_{Ar}). For C₂₂H₂₅N₃O₂ calculated C 72.7 H 6.9 N 11.6 found C 72.7 H 7.0 N 11.8%.

4.10. N,N'-bis[(2-hydroxy-3-methoxyphenyl)methyl]-N'-[(2-hydroxyphenyl)methyl]ethane-1,2-diamine (3c)

Methanol (20 cm³), N,N'-bis[(2-hydroxy-3-methoxyphenyl)methyl]ethane-1,2-diamine (1b) 0.830 g (2.5 mmol) and salicylaldehyde 0.3 cm³ (2.5 mmol) were introduced into

a round-bottomed flask. The reaction mixture was kept under stirring for 1.5 h at room temperature. Trichloroacetic acid 0.409 g (2.5 mmol) was added while the reaction flask was in an ice-salt bath. Small portions of sodium borohydride 0.154 g (4 mmol) were introduced. Gas evolution was observed. Initially the reaction was carried out in an ice bath for 2 h, then at room temperature for a following hour. All the volatiles were evaporated on a rotary evaporator and the resulting oily, pale pink residue was dissolved in 5 cm³ chloroform, washed with water (10 cm³) and the aqueous layer was extracted with chloroform (3 × 5 cm³). The organic phases were combined, dried over anhydrous magnesium sulfate and evaporated on a rotary evaporator resulting in crude product (0.915 g, 83%). A portion of the product (0.200 g) was purified by column chromatography (MeOH/CHCl₃ 1:9) to give pure product (0.174 g, 0.397 mmol, 15%) as a pale pink solid (purification yield 87%, total yield for pure product 72%). ¹H NMR (400 MHz, CDCl₃): δ 2.68 (t, 2H, J = 6 Hz, CH₂-CH₂-NH), 2.82 (t, 2H, J = 6 Hz, N-CH₂-CH₂), 3.72 (m, 4H, Ar-CH₂-NH), 3.85 (s, 6H, CH₃-O), 3.86 (s, 2H, Ar-CH₂-N), 6.54 (d, 1H, J = 7.6 Hz, Ar), 6.70 (t, 1H, J = 7.6 Hz, Ar), 6.76–6.80 (m, 6H, Ar), 6.98 (d, 1H, J = 7.2 Hz, Ar), 7.14 (td, 1H, J = 8.0, 1.6 Hz, Ar) ¹³C{¹H} NMR (400 MHz, CDCl₃): δ 45.0 (CH₂-CH₂-NH), 50.5 (N-CH₂-CH₂), 51.8, 54.2, 55.2, 55.8 (CH₃O), 55.9 (CH₃O), 57.5 (C_{Ar}), 110.7 (C_{Ar}), 110.8 (C_{Ar}), 116.2 (C_{Ar}), 118.7 (C_{Ar}), 119.3 (C_{Ar}), 121.1 (C_{Ar}), 122.34 (C_{Ar}), 122.4 (C_{Ar}), 122.5 (C_{Ar}), 123 (C_{Ar}), 128.9 (C_{Ar}), 129.2 (C_{Ar}), 144.7 (C_{Ar}), 146.8 (C_{Ar}), 146.9 (C_{Ar}), 147.6 (C_{Ar}), 157.0 (C_{Ar}) MS-ESI (m/z): 439.6 [M + H]⁺, 437.5 [M - H]⁺. HRMS [M + H]⁺: for C₂₅H₃₁N₂O₅ calculated 439.2226, found 439.2233, For C₂₅H₃₀N₂O₅ calculated C 68.5 H 6.9 N 6.4 found C 68.1 H 7.0 N 6.9%.

4.11. N,N'-Bis[(2-hydroxy-3-methoxyphenyl)methyl]-N'-(2-pyridyl)methyl]ethane-1,2-diamine (3d)

Anhydrous methanol (30 cm³), N,N'-bis[(2-hydroxy-3-methoxyphenyl)methyl]ethane-1,2-diamine (1b) 0.830 g (2.5 mmol) and 2-pyridine carboxyaldehyde 0.25 cm³ (2.5 mmol) were introduced into a round-bottomed flask. The mixture was kept under stirring for 1.5 h at room temperature. Then the reaction mixture was cooled at an ice-salt bath while stirring. Trifluoroacetic acid 0.38 cm³ (4 mmol) was added to the reaction mixture and next sodium cyanoborohydride 0.317 g (5 mmol) was introduced in small portions. The reaction mixture was kept in ice bath for 2 h, then at room temperature for 24 h. All the volatiles were evaporated on a rotary evaporator and the resulting light brown oily residue was dissolved in 5 cm³ chloroform, washed with water (10 cm³) and the aqueous layer was extracted with chloroform (3 × 5 cm³). The organic phases were combined, dried over anhydrous magnesium sulfate and evaporated on a rotary evaporator resulting in crude product 0.962 g. The product was purified by column chromatography (MeOH/CHCl₃ 1:9) to give pure product as a yellow oil (0.683 g, 1.61 mmol, 64%). ¹H NMR (400 MHz, CDCl₃): δ 2.65 (t, 2H, J = 5.7 Hz, CH₂-CH₂-NH), 2.74 (t, 2H, J = 5.7 Hz, N-CH₂-CH₂), 3.72 (s, 4H, Ar-CH₂-NH), 3.81 (s, 3H, CH₃-O), 3.87 (s, 8H, CH₃-O, Ar-CH₂-N), 6.46 (d, 1H, J = 7.5 Hz, Ar), 6.66 (dd, 2H, J = 8.0, 8.0 Hz, Ar), 6.72–6.77 (m, 2H, Ar), 6.83 (dd, 1H, J = 8.0, 1.6 Hz, Ar), 7.22 (m, 2H, Ar), 7.67

(td, 1H, J = 7.6, 1.6 Hz, Ar), 8.61 (d, 1H, J = 4.9 Hz, Ar-py), ¹³C{¹H} NMR (400 MHz, CDCl₃): δ 45.2 (CH₂-CH₂-NH), 50.7 (N-CH₂-CH₂), 52.1, 55.2, 55.8 (CH₃O), 55.9 (CH₃O), 57.3, 59.2 (C_{Ar}), 110.8 (C_{Ar}), 111.3, 118.5 (C_{Ar}), 118.7 (C_{Ar}), 120.8 (C_{Ar}), 122.0 (C_{Ar}), 122.4 (C_{Ar}), 122.9 (C_{Ar}), 123.2 (C_{Ar}), 136.9 (C_{Ar}), 146.5 (C_{Ar}), 147.2 (C_{Ar}), 147.8 (C_{Ar}), 148.2, 149.0, 157.5 (C_{Ar}) MS-ESI (m/z): 424.8 [M + H]⁺, 422.7 [M - H]⁺, 848.1 [2M + 2H]⁺, HRMS [M + H]⁺: for C₂₄H₃₀N₃O₄ calculated 424.2236, found 424.2216, For C₂₄H₂₉N₃O₄ calculated C 68.1 H 6.9 N 9.9 found C 67.8 H 7.2 N 10.2%.

4.12. N,N'-Bis[(2-hydroxynaphthyl)methyl]-N'-(2-pyridyl)methyl]ethane-1,2-diamine (3e)

Methanol (5 cm³), 2-naphthol 0.29 g (4 mmol), (0.30 g, 2 mmol) N-(pyridil-2-methyl)ethane-1,2-diamine (4) and 0.3 cm³ (4 mmol) formaldehyde 37% were introduced into a round-bottomed flask. The mixture was warmed up and a precipitate appeared. The reaction mixture was kept under stirring for 42 h at room temperature. The product was filtered off and dried (0.658 g, 1.41 mmol, 71%). ¹H NMR (400 MHz, CDCl₃): δ 2.45 (m, 4H, CH₂-CH₂-NH and N-CH₂-CH₂), 3.90 (s, 2H, Py-CH₂-N), 4.10 (s, 2H, Naphthyl-CH₂-N), 4.18 (s, 2H, Naphthyl-CH₂-NH), 6.85 (m, 2H, Ar), 7.35–7.77 (m, 9H, Ar), 8.02 (m, 4H, Ar), 8.39 (m, 1H Ar), ¹³C{¹H} NMR (400 MHz, CDCl₃): δ 46.2 (Ar-CH₂-N), 46.9 (CH₂-CH₂-NH), 54.0 (Ar-CH₂-NH), 55.7 (N-CH₂-CH₂), 62.5 (Py-CH₂-N), 115.2 (C_{Ar}), 118.9 (C_{Ar}), 120.3 (C_{Ar}), 121.0 (C_{Ar}), 122.5 (C_{Ar}), 124.0 (C_{Ar}), 126.3 (C_{Ar}), 128.3 (C_{Ar}), 128.7 (C_{Ar}), 131.3 (C_{Ar}), 139.3 (C_{Ar}), 148.7 (C_{Ar}), 153.4 (C_{Ar}), 157.8 (C_{Ar}), MS-ESI (m/z): 464 [M + H]⁺, 462 [M - H]⁺, For C₃₀H₂₉N₃O₂ calculated C 77.7 H 6.3 N 9.1 found C 77.5 H 6.6 N 9.5%.

4.13. Iron(III) complex 4a [Fe(3a)]

Methanol (5 cm³), and N,N,N'-tris[(2-hydroxyphenyl)methyl]ethane-1,2-diamine (3a) 0.416 g (1.1 mmol) were introduced into a round-bottom flask. Ferric chloride 0.163 g (1 mmol in 5 cm³ methanol) was added while stirring. The mixture turned dark purple. The reaction mixture was kept under stirring for 1 h at room temperature then an aqueous solution of sodium hydroxide (0.5 M: 0.132 g, 3.3 mmol NaOH in 6.6 cm³ water) was introduced. This resulted in dark brown solution. The reaction mixture was stirred for following 0.5 h and then moved to fridge for 24 h. All the volatiles were evaporated on a rotary evaporator. Crude product was purified by column chromatography (MeOH/CHCl₃ 1:1) to give pure product (0.289 g, 0.670 mmol, 67%). IR (cm⁻¹): 3586 w (v_{N-H}), 1625 mw, 1595 mw (v_{c=c}), 1479 mw, 1451 mw (δ_{c-H}), 1283 m (v_{c-N}), 1092 s (v_{c-o}), 752 s for 1,2-disubstituted benzene ring. MS-ESI (m/z): 454.3 [M + Na]⁺, 430.3 [M - H]⁺. HRMS [M + Na]⁺: for C₂₃H₂₃FeN₂O₃Na calculated 454.0942, found 454.0947, For C₂₃H₂₃N₂O₃Fe calculated C 64.1 H 5.4 N 6.5 found C 64.0 H 5.5 N 6.7%.

4.14. Iron(III) complex 4b [Fe(3b)]ClO₄

Methanol (5 cm³), N,N'-bis[(2-hydroxyphenyl)methyl]-N'-(pyridyl)methyl]ethane-1,2-diamine (3b) 0.199 g (0.55 mmol) were introduced into a round-bottom flask. Iron(III)

perchlorate 0.186 g (0.50 mmol in 5 cm³ of methanol) was added while stirring. The mixture turned dark purple. The reaction was kept under stirring for 1.5 h at room temperature, next an aqueous solution of sodium hydroxide (0.5 M: 0.044 g, 1.1 mmol NaOH in 2.2 cm³ water) was introduced. The mixture changed color to dark brown. After stirring for next hour it was moved to fridge for 24 h. All the volatiles were evaporated on a rotary evaporator. The residue was washed with water (3 × 5 cm³), dried and then with diethyl ether (3 × 5 cm³) and dried again resulting in pure product (0.181 g, 0.350 mmol, 70%). *IR* (cm⁻¹): 3599 w (v_{N-H}), 2920 w (v_{C-H}), 1593 m, 1567 mw (v_{C=C}), 1477 m, 1450 m (δ_{C-H}), 1267 m (v_{C-N}), 1085 m (v_{C-O}), 754 s for 1,2-disubstituted benzene ring. *MS-ESI* (m/z): 417 [M-ClO₄]⁺. *HRMS* [M]⁺: for C₂₂H₂₃FeN₃O₂ calculated 417.1139, found 417.1106, For C₂₂H₂₃N₃O₆ClFe calculated C 51.1 H 4.5 N 8.1 found C 51.0 H 4.7 N 8.5%.

4.15. Iron(III) complex 4c [Fe(3c)]

Methanol 5 cm³, *N,N'*-bis[(2-hydroxy-3-methoxyphenoxy)methyl]-*N'*-(2-hydroxyphenyl)methyl]ethane-1,2-diamine (3c) 0.109 g (0.25 mmol) were introduced into a round-bottom flask. Iron(III) perchlorate 0.094 g (0.25 mmol in 5 cm³ of methanol) was added while stirring. The mixture turned dark purple. The reaction was kept under stirring for 1.5 h at room temperature, next an aqueous solution of sodium hydroxide (0.5 M: 0.03 g, 0.75 mmol NaOH in 1.5 cm³ water) was introduced. After stirring for next hour it was moved to fridge for 24 h. All the volatiles were evaporated on a rotary evaporator. Crude product was purified by column chromatography (MeOH/CHCl₃ 1:2) to give pure product (0.095 g, 0.193 mmol, 76%). *IR* (cm⁻¹): 3399 w (v_{N-H}), 2919 w (v_{C-H}), 2849 w (v_{C-Oalif}), 1596 w, 1574 w(v_{C=C}), 1476 ms (δ_{C-H}), 1239 ms (v_{C-N}), 1077 s (v_{C-O}), for 1,2,3-trisubstituted benzene ring: 852 m, 764 m, 739 ms. *MS-ESI* (m/z): 492 [M+H]⁺, 514 [M+Na]⁺. *HRMS* [M+Na]⁺: for C₂₅H₂₇N₂O₅FeNa calculated 514.1168, found 514.1180, For C₂₅H₂₇N₂O₅Fe calculated C 61.1 H 5.5 N 5.7 found C 60.9 H 5.5 N 5.9%.

4.16. Iron(III) complex 4d Na[Fe(3d)₂]

Methanol 5 cm³, *N,N'*-bis[(2-hydroxy-3-methoxyphenyl)methyl]-*N'*-(2-pyridyl)methyl]ethane-1,2-diamine (3d) 0.200 g (0.47 mmol) were introduced into a round-bottom flask. Iron(III) perchlorate 0.177 g (0.47 mmol in 5 cm³ of methanol) was added while stirring. The mixture turned dark purple. The reaction was kept under stirring for 1.5 h at room temperature, next an aqueous solution of sodium hydroxide (0.5 M: 0.04 g, 0.94 mmol NaOH in 1.5 cm³ water) was introduced. After stirring for next hour it was moved to fridge for 24 h. All the volatiles were evaporated on a rotary evaporator. Crude product was purified by column chromatography on reversed phase (CH₃CN/H₂O 1:1) to give pure product (0.125 g, 0.217 mmol, 46%). *IR* (cm⁻¹): 3241 w (v_{N-H}), 2930 w (v_{C-H}), 2058 (v_{C-Oalif}), 1606 mw, 1569 mw (v_{C=C}), 1475 m, 1459 m (δ_{C-H}), 1241 m (v_{C-N}), 1079 m (v_{C-O}), 856 ms, 764 m, 740 ms s for 1,2,3-trisubstituted benzene ring. *MS-ESI* (m/z): 477 [M-ClO₄]⁺. *HRMS* [M]⁺: for C₂₄H₂₇N₂O₅ calculated 477.1350, found 477.1309, For C₂₄H₂₇N₃O₈ClFe calculated C 50.0 H 4.7 N 7.3 found C 49.8 H 4.8 N 7.6%.

4.17. Iron(III) complex 4e [Fe(3e)]Cl

Methanol (5 cm³), *N,N'*-bis[(2-hydroxynaphthyl)methyl]-*N'*-(2-pyridyl)methyl]ethane-1,2-diamine (3e) 0.050 g (0.108 mmol) were introduced into a round-bottom flask. Ferric chloride 0.018 g (0.108 mmol in 5 cm³ of methanol) was added while stirring. The reaction was conducted under reflux for 2 h. Initially, the reaction mixture turned dark green color and after 10 min the solution became dark purple color. After 2 h the reaction flask was cooled and allowed in the fridge for 24 h. All the volatiles were evaporated on a rotary evaporator. Crude product was purified by column chromatography on reverse phase (CH₃CN: H₂O 4:1) to give pure product (0.029 g, 0.052 mmol, 48%). *MS-ESI* (m/z): 517 [M-Cl]⁺, *HRMS* [M-Cl]⁺: for C₃₀H₂₇FeN₃O₂ calculated 517.1453, found 517.1452, For C₃₀H₂₇N₃O₂ClFe calculated C 65.2 H 4.9 N 7.6 found C 65.0 H 5.2 N 7.9%.

4.18. N-(2-Pyridylmethyl)ethane-1,2-diamine (4)

Ethanol (25 cm³), 3.34 ml of ethane-1,2-diamine (50 mmol) and sodium carbonate 0.84 g (10 mmol) were added to a round bottom flask. Then slowly added dropwise a solution of 2-(chloromethyl)pyridine hydrochloride (1:1) in 10 cm³ of ethanol (0.82 g, 5 mmol). The reaction mixture was kept under stirring for 18 h at room temperature. The product was purified by column chromatography (1:9 MeOH/CHCl₃ + 1% NH₃ 25% solution) to give pure product (0.568 g, 3.75 mmol, 75%). *1H NMR* (300 MHz, CDCl₃): δ 2.73 (t, 2H, N-CH₂, J = 6 Hz), 2.84 (t, 2H, CH₂-N, J = 6 Hz), 3.92 (s, 2H, CH₂-py), 7.15–7.19 (m, 1H, Ar), 7.30–7.33 (m, 1H, Ar), 7.62–7.68 (m, 1H Ar), 8.55 (d, 1H, Ar, J = 7.5 Hz), *13C*{¹H} *NMR* (300 MHz, CDCl₃): δ 41.89 (Ar-CH₂), 52.32 (N-CH₂), 55.18 (CH₂-NH), 122.18 (C_{Ar}), 122.51 (C_{Ar}), 136.73 (C_{Ar}), 143.39(C_{Ar}), 159.32 (C_{Ar}), For C₈H₁₃N₃ calculated C 63.5 H 8.7 N 27.8 found C 63.2 H 8.9 N 27.8%.

4.19. *N,N*-Bis(2-hydroxy-1-naphthylmethyl)-2-aminoethanol (5) described in Adamek's patent

(Adamek and Bobulova, 1968). Methanol (20 cm³), 2-naphthol 7.2 g (50 mmol), 2-aminoethanol 1.5 cm³ (10 mmol) and formaldehyde 37% 1.6 cm³ (20 mmol) were introduced into a round-bottomed flask. Mixture warmed up and a pale orange precipitate appeared. Reaction mixture was kept under stirring for 48 h at room temperature. The product was filtered off on fritted funnel and dried (2.99 g, 7.98 mmol 80%). mp = 124–126 °C, *1H NMR* (300 MHz, CDCl₃): δ 2.89 (t, 2H, N-CH₂, J = 5.3 Hz), 3.89 (t, 2H, CH₂-OH, J = 5.3 Hz), 4.38 (s, 4H, Ar-CH₂), 7.11 (d, 2H, Ar, J = 8.8 Hz), 7.30 (t, 2H, Ar, J = 7.7 Hz), 7.50 (t, 2H Ar J = 7.7 Hz), 7.68 (d, 2H, Ar, J = 8.8 Hz), 7.74 (d, 2H, Ar, J = 7.7 Hz), 8.01 (d, 2H, Ar, J = 8.8 Hz) *13C*{¹H} *NMR* (300 MHz, CDCl₃): δ 50.79 (Ar-CH₂), 51.9 (N-CH₂), 60.5 (CH₂-OH), 112.7 (C_{Ar}), 118.8 (C_{Ar}), 121.3 (C_{Ar}), 122.7 (C_{Ar}), 126.7 (C_{Ar}), 128.8 (C_{Ar}), 128.9 (C_{Ar}), 129.9 (C_{Ar}), 133.3 (C_{Ar}), 154.8 (C_{Ar}), *HRMS* [M+H]⁺: for C₂₄H₂₄NO₃ calculated 374.1743, found 374.1749, For C₂₄H₂₃NO₃ calculated C 77.2 H 6.2 N 3.8 found C 77.0 H 6.3 N 3.9%.

4.20. *N,N*-Bis(2-hydroxy-1-naphthylmethyl)-2-chloroethanamine (6)

Dichloromethane (10 cm³) and *N,N*-bis(2-hydroxy-1-naphthylmethyl)-2-aminoethanol (5) 1.37 g (3.66 mmol) were introduced into a round-bottomed flask. Freshly distilled thionyl chloride 0.3 cm³ (4.66 mmol) was added dropwise while stirring. Dark tar separated out from the reaction mixture. After 24 h of stirring at room temperature all of the volatiles were removed *in vacuo*. After the addition of saturated solution of sodium carbonate (10 ml), the mixture was stirred for 24 h, then extracted with dichloromethane (3 × 20 cm³). The combined extracts were dried with anhydrous MgSO₄ and the solvent was evaporated *in vacuo*. The crude product was purified by column chromatography (MeOH/CHCl₃ 1:9) to give pure product as a gray powder (0.70 g, 1.78 mmol, 49%) ¹H NMR (300 MHz, CDCl₃): δ 3.12 (t, 2H, N-CH₂, J = 6.7 Hz), 3.71 (t, 2H, CH₂-Cl, J = 6.7 Hz), 4.40 (s, 4H Ar-CH₂), 7.11 (d, 2H, Ar, J = 8.9 Hz), 7.32 (t, 2H, Ar, J = 7.6 Hz) 7.51 (t, 2H, Ar, J = 7.6 Hz), 7.68 (d, 2H, Ar, J = 8.9 Hz), 7.75 (d, 2H, J = 7.9 Hz), 7.97 (d, 2H, Ar, J = 8.6 Hz) ¹³C{¹H} NMR (300 MHz, CDCl₃): δ 46.3 (N-CH₂), 50.5 (Ar-CH₂), 55.5 (CH₂-Cl), 118.3 (C_{Ar}), 120.8 (C_{Ar}), 121.6 (C_{Ar}), 123.0 (C_{Ar}), 126.4 (C_{Ar}), 126.8 (C_{Ar}), 128.9 (C_{Ar}), 129.0 (C_{Ar}), 130.9 (C_{Ar}), 154.2 (C_{Ar}), HRMS [M+H]⁺: for C₂₄H₂₃ClNO₂ calculated 392.1427, found 392.1417, For C₂₄H₂₂NO₂Cl calculated C 73.6 H 5.7 N 3.6 found C 73.6 H 5.8 N 3.9%.

4.21. *N*-(Pyridyl)methyl]-*N,N*-bis(2-hydroxy-1-naphthylmethyl)amine (7) (Conditions for the synthesis of compound 3e')

Ethanol (4 cm³), 1.03 ml of 1-(2-pyridylmethyl)amine (10 mmol) were added to a round bottom flask. Then slowly added dropwise a solution of *N,N*-bis(2-hydroxy-1-naphthylmethyl)-2-chloroethanamine (6) 4 cm³ of ethanol (0.39 g, 1 mmol) the reaction mixture was kept under stirring for 48 h at room temperature. The crude product was purified by column chromatography (1:9 MeOH/CHCl₃ + 1% NH₃ 25% solution) to isolate pure product (7) as a yellow oil (0.217 g, 0.516 mmol, 52%). ¹H NMR (300 MHz, CD₃COCD₃): δ 3.89 (s, 2H, CH₂-py), 4.34 (s, 4H, CH₂-naphthol), 6.70 (d, 1H, Ar), 7.16–7.87 (m, 14H, Ar), 8.65 (d, 2H, Ar), MS-ESI (m/z): 421 [M+H]⁺, 443 [M+Na]⁺, For C₂₈H₂₄N₂O₂ calculated C 80.0 H 5.5 N 6.7 found C 79.6 H 5.6 N 6.5%.

4.22. *N,N*-Bis[1-(2-hydroxynaphthyl)methyl]-2,2-diethoxyethanamine (8)

Methanol (8 cm³) and 2-naphthol 2.88 g (20 mmol) and formaldehyde 37% 1.64 cm³ (20 mmol) were introduced into a round-bottomed flask. 2,2-diethoxyethanamine 1.46 cm³ (10 mmol) was added dropwise while stirring. Dark tar separated out from the reaction mixture. After 2 h precipitate was observed. Reaction mixture was kept under stirring for 48 h at room temperature. The product was filtered on fritted funnel, washed with cold methanol and dried (3.16 g, 6.87 mmol, 69%). ¹H NMR (300 MHz, CDCl₃): δ 1.19 (t, 6H, O-CH₂-CH₃, J = 7.2 Hz), 2.80 (d, 2H, CH-CH₂-N, J = 5.4 Hz), 3.42 (q, 2H, O-CH₂-CH₃, J = 6.9 Hz), 3.60

(q, 2H, O-CH₂-CH₃, J = 6.9 Hz), 4.34 (s, 4H, Ar-CH₂), 4.69 (t, 1H, N-CH₂-CH₃, J = 5.4 Hz), 7.13 (d, 2H, Ar, J = 9 Hz), 7.29 (td, 2H, Ar, J = 7.2, 1.2 Hz), 7.48 (td, 2H, Ar, J = 7.2, 1.2 Hz), 7.73 (m, 4H, Ar), 7.99 (d, Ar, 2H, J = 9 Hz) ¹³C{¹H} NMR (300 MHz, CDCl₃): δ 15.1 (O-CH₂-CH₃), 51.3 (Ar-CH₂-N), 54.4 (O-CH₂), 63.0 (CH₂-N), 101.1 (N-CH₂-CH₃), 113.1 (C_{Ar}), 119.0 (C_{Ar}), 121.6 (C_{Ar}), 122.9 (C_{Ar}), 126.8 (C_{Ar}), 129.0 (C_{Ar}), 130.1 (C_{Ar}), 133.5 (C_{Ar}), 155.1 (C_{Ar}), HRMS [M+H]⁺: for C₂₈H₃₂NO₄ calculated 446.2318, found 446.2313, For C₂₈H₃₁NO₄ calculated C 75.5 H 7.0 N 3.1 found C 75.3 H 7.3 N 3.4%.

Acknowledgements

This work was supported by Polish National Science Center (NCN); Decision No.:DEC-2012/07/B/ST5/03157. We would like to thank Prof. M. Kubicki and Dr. G. Dudkiewicz from A. Mickiewicz University in Poznań for the X-ray measurements. M. Wyskocka and R. Komor acknowledge DoktoRIS – Scholarship program for innovative Silesia co-financed by the European Union Funds.

Appendix A. Supplementary data

Supplementary data associated with this article can be found, in the online version, at <http://dx.doi.org/10.1016/j.arabjc.2014.11.009>.

References

- Adamek, M., Bobulova, P., 1968. Způsob výroby nové dusíkaté báze tj. *N,N*-bis(2-hydroxy-1-naftylmetyl)etanolaminu, CZ Patent 128430.
- Bloembergen, N., 1957. Proton relaxation times in paramagnetic solutions. J. Chem. Phys. 27, 572.
- Caravan, P., 2009. Protein-targeted gadolinium-based magnetic resonance imaging (MRI) contrast agents: design and mechanism of action. Acc. Chem. Res. 42, 851–862.
- Caravan, P., Ellison, J.J., McMurry, T.J., Lauffer, R.B., 1999. Gadolinium(III) chelates as MRI contrast agents: structure, dynamics, and applications. Chem. Rev. 99, 2293–2352.
- Dean, R.K., Fowler, C.I., Hasan, K., Kerman, K., Kwong, P., Trudel, S., Leznoff, D.B., Kraatz, H.B., Dawe, L.N., Kozak, C.M., 2012. Magnetic, electrochemical and spectroscopic properties of iron(III) amine-bis (phenolate) halide complexes. Dalton Trans. 41, 4806–4816.
- Dorazio, S.J., Morrow, J.R., 2012. The development of iron(II) complexes as ParaCEST MRI contrast agents. Eur. J. Inorg. Chem., 2006–2014.
- Report on Critical Raw Materials for the EU, 2014. European Commission.
- Fife, T.H., Hutchins, J.E.C., Pellino, A.M., 1978. General acid catalyzed imidazolidine hydrolysis. Hydrolysis of 2-(tert-butyl)-*N,N'*-dimethyl-1,3-imidazolidine and 2-(*p*-methoxyphenyl)-*N*-isopropyl-*N'*-phenyl-1,3-imidazolidine. J. Am. Chem. Soc. 100, 6455–6462.
- Geraldes, C.F.G.C., Laurent, S., 2009. Classification and basic properties of contrast agents for magnetic resonance imaging. Contrast Media Mol. Imaging 4, 1–23.
- Hasserodt, J., 2012. Magnetogenic probes that respond to chemical stimuli in an off-on mode. New J. Chem. 36, 1707–1712.
- Hermann, P., Kotek, J., Kubíček, V., Lukeš, I., 2008. Gadolinium(III) complexes as MRI contrast agents: ligand design and properties of the complexes. Dalton Trans., 3027–3047.

Kivelitz, D., Gehl, H.B., Heuck, A., Krahe, T., Taupitz, M., Lodemann, K.P., Hamm, B., 1999. Ferric ammonium citrate as a positive bowel contrast agent for MR imaging of the upper abdomen: safety and diagnostic efficacy. *Acta Radiol.* 40, 429–435.

Kümmerer, K., Helmers, E., 2000. Hospital effluents as a source of gadolinium in the aquatic environment. *Environ. Sci. Technol.* 34, 573–577.

Kuźnik, N., Stavila, V., Allali, M., Stortz, Y., Maurin, P., Hasserodt, J., 2008. Spin-state variable, iron-based, enzyme-responsive MRI contrast agents: evaluation of two molecule candidates employing distinct auto-immutable architectures. *Abstr. Pap. Am. Chem. Soc.*, 343-INOR.

Kuźnik, N., Chrobaczyński, A., Mika, M., Miler, P., Komor, R., Kubicki, M., 2012. A new class of bioactivatable self-immutable *N,O*-ligands. *Eur. J. Med. Chem.* 52, 184–192.

Kuźnik, N., Jewua, P., Oczek, L., Kozowicz, S., Grucela, A., Domagała, W., 2014. EHPG iron(III) complexes as potential contrast agents for MRI. *Acta Chim. Slov.* 61, 87–93.

Lauffer, R.B., 1987. Paramagnetic metal complexes as water proton relaxation agents for NMR imaging: theory and design. *Chem. Rev.* 87, 901–927.

Lauffer, R.B., Vincent, A.C., Padmanabhan, S., Villringer, A., Saini, S., Elmaleh, D.R., Brady, T.J., 1987. Hepatobiliary MR contrast agents: 5-substituted iron-EHPG derivatives. *Magn. Reson. Med.* 4, 582–590.

Major, J.L., Meade, T.J., 2009. Bioresponsive, cell-penetrating, and multimeric MR contrast agents. *Acc. Chem. Res.* 42, 893–903.

Margerum, D.W., Cayley, G.R., Weatherburn, D.C., Pagenkopf, D.W., 1978. In: Martell, A.E. (Ed.), *Coordination Chemistry*. American Chemical Society, Washington D.C..

Marvilliers, A., Poussereau, S., 2002. Mononuclear iron III complex with the pentadentate ligand *N,N'*-bis (2-hydroxybenzyl), *n*-(2-pyridylmethyl) ethane-1,2-diamine. Synthesis and characterisation. *J. Nat.* 14, 97–102.

Pierre, V.C., Allen, M.J., Caravan, P., 2014. Contrast agents for MRI: 30+ years and where are we going? *J. Biol. Inorg. Chem.* 19, 127–131.

Que, E.L., Chang, C.J., 2009. Responsive magnetic resonance imaging contrast agents as chemical sensors for metals in biology and medicine. *Chem. Soc. Rev.* 39, 51–60.

Richardson, N., Davies, J.A., Raduchel, B., 1999. Iron(III)-based contrast agents for magnetic resonance imaging. *Polyhedron* 18, 2457–2482.

Schmitt, H., Lomoth, R., Magnuson, A., Park, J., Fryxelius, J., Kritikos, M., Mårtensson, J., Hammarström, L., Sun, L., Åkermark, B., 2002. Synthesis, redox properties, and EPR spectroscopy of manganese(III) complexes of the ligand *N,N*-bis(2-hydroxybenzyl)-*N'*-2-hydroxybenzylidene-1,2-diaminoethane: formation of mononuclear, dinuclear, and even higher nuclearity complexes. *Chem. Eur. J.* 8, 3757–3768.

Schwert, D., Davies, J., Richardson, N., 2002. Contrast agents I; non-gadolinium-based MRI contrast agents. *Top. Curr. Chem.*, 165–199.

Searcey, M., Grewal, S.S., Madeo, F., Tsoungas, P.G., 2003. A mild procedure for the production of secondary amines from oximes and benzisoxazoles. *Tetrahedron Lett.* 44, 6745–6747.

Touti, F., Maurin, P., Hasserodt, J., 2013. Magnetogenesis under physiological conditions with probes that report on (bio-)chemical stimuli. *Angew. Chem., Int. Ed.* 52, 4654–4658.

Wang, Y.X., 2011. Superparamagnetic iron oxide based MRI contrast agents: current status of clinical application. *Quant. Imaging. Med. Surg.* 1, 35–40.

Yerram, P., Saab, G., Karuparthi, P.R., Hayden, M.R., Khanna, R., 2007. Nephrogenic systemic fibrosis: a mysterious disease in patients with renal failure—role of gadolinium-based contrast media in causation and the beneficial effect of intravenous sodium thiosulfate. *Clin. J. Am. Soc. Nephrol.* 2, 258–263.